

# Hydrothermal Ageing Effects on the Coprecipitated Mullite-Alumina Composite Precursor

M. Zhou, J. M. F. Ferreira, A. T. Fonseca & J. L. Baptista

Department of Ceramic and Glass Engineering, University of Aveiro, 3810 Aveiro, Portugal

(Received 20 October 1996; accepted 17 January 1997)

## Abstract

*Hydrothermal ageing experiments were performed on a mullite suspension obtained by a coprecipitation method to study its effects on the electrophoretic behaviour and morphology of the particles in suspension. The changes in hydration degree, and chemical environments of silicon ions and aluminium ions were also studied. With the increase in the ageing time, the isoelectric point (IEP) of the particles surface gradually decreased from pH 8.2, for the freshly precipitated powder, to pH 5.8 after the suspension has been refluxed at 100°C for 24 hours. This shift in IEP was attributed to a depolymerization and dissolution process of silicon-containing species and its precipitation on the surface of the particles present in the aged suspensions. The hydration degree of the precursor was reduced as shown by the weight changes in the TG analysis. These phenomena were enhanced by autoclave ageing at 230°C which transformed all bayerite into boehmite. These transformations were accompanied by some replacement of  $\equiv\text{Si}-\text{O}-\text{Si}\equiv$  bonds by  $\equiv\text{Si}-\text{O}-\text{Al}\equiv$  bonds and smoothing of the particle surface.*  
© 1997 Elsevier Science Limited.

## 1 Introduction

Mullite has been studied for certain structural applications because of its excellent phase stability, low thermal conductivity, excellent creep resistance and high temperature strength retention as compared to other engineering ceramic materials.<sup>1,2</sup> There are several ways to prepare mullite precursor. One of them is the coprecipitation method by which diphasic precursors with Al-components and Si-components mixed in a nanometer scale could

be derived. In our previous work,<sup>3</sup> freshly prepared precursors exhibited a total weight loss of about 35%, which was due to its high degree of hydration. As a result, an attempt to prepare green bodies by directly slip casting from the precipitated and washed slurries obtained only a moderate success.<sup>4</sup> It was also observed that the dispersion ability of the slurries and the mixing degree of the two components were influenced by the ageing time at room temperature. Direct colloidal processing of ceramic material precursors obtained by Sol-Gel methods are limited by strong agglomeration, big weight losses and high shrinkage during drying and the initial stages of the thermal treatment of the green body, which would cause inevitable damage to the ceramic bodies, such as cracks and deformation. Changing the morphology, the state of aggregation and the hydration state of the precursors, and improving the dispersion ability of the particles in the suspension, are essential to obtain green bodies that behave well during sintering.

In the present work, hydrothermal ageing, both at 100 and 230°C, was carried out to study the ageing effects on the hydration state of the precursor, and also the electrophoretic behaviour, morphology and size distribution of the particles in suspension. The ageing effect on the chemical environments of the aluminium ions and silicon ions was also studied. The objective was to understand how the properties of the precursor could be modified, from the initial stage of its preparation, in a way that would improve direct colloidal processability of the obtained slurries.

## 2 Experimental

The suspensions with 10 vol% excess alumina over stoichiometric mullite composition were prepared

by the coprecipitation method reported earlier.<sup>3,4</sup> The single alumina-containing suspension and single silica-containing suspension were prepared by adding an  $\text{AlCl}_3$  solution or a silica sol derived from sodium metasilicate, respectively, to an ammonium hydroxide ( $\text{NH}_4\text{OH}$ ) solution. The cationic acidic solutions were sprayed with compressed air (from a glass nozzle) into the diluted  $\text{NH}_4\text{OH}$  solution maintained at  $\text{pH}=8.5$  under strong mechanical agitation. The pH was controlled and adjusted automatically by using a pH meter (Cole-Palmer pH/ORP controller, model 5652-10) coupled with a diaphragm-type pump (Cole-Palmer metering pump, Series 7142) which drops  $\text{NH}_4\text{OH}$  solution onto the precipitating solution. The precipitated suspensions were filtered and redispersed into distilled water several times to remove the  $\text{Cl}^-$  and  $\text{Na}^+$ . The ageing experiments were carried out by refluxing at  $100^\circ\text{C}$  under 1 atm pressure in air for 3, 7, 12 and 24 h and by using an autoclave at  $230^\circ\text{C}$  for 72 h. Some parts of the suspensions (unaged, aged at  $100^\circ\text{C}$  for 24 h and aged in autoclave at  $230^\circ\text{C}$  for 72 h) were filtered and dried in air at room temperature for 3 days and at  $100^\circ\text{C}$  for 10 h. The dried powders were analysed by X-Ray Diffraction (XRD) with an X-ray diffractometer (Model XDMAX, Rigaku/USA, Inc., Danvers, Ma) by using  $\text{CuK}\alpha$  radiation in the  $10\text{--}70^\circ$   $2\theta$ -range at a scanning speed of  $2^\circ$   $2\theta$   $\text{min}^{-1}$ , and thermogravimetric analysis (TGA) (Model LINSEIS/THERMAL, LINSEIS, Inc., Princeton Junction, NJ) at a heating rate of  $10^\circ\text{C min}^{-1}$ , up to  $1400^\circ\text{C}$ .

A computer-controlled Malvern AZ-6004 Zeta-sizer (Malvern Instruments, Malvern, UK) was used for particle size distribution analysis and zeta-potential measurements. The concentrated suspensions were diluted and dispersed in 0.001 M NaCl solution and the pH of the suspensions was adjusted by adding 0.001 M HCl or NaOH solutions.<sup>4</sup>

The morphology of the particles in the unaged and refluxed aged suspensions was observed by Scanning Electron Microscopy (SEM) (Model S4100-1, Hitachi, Ltd, Tokyo, Japan). Samples for these observations were prepared by dropping the dilute suspensions on the surface of thin glass pellets and drying at room temperature, followed by depositing a carbon film on them. The MAS NMR spectra of the dried unaged and the autoclave aged powders were recorded on a Bruker MSL 400P spectrometer. Samples were spun at the magic-angle in a zirconia rotor.  $^{29}\text{Si}$  MAS NMR spectra were recorded at 79.494 MHz using  $45^\circ$  radiofrequency pulses with an interpulse delays of 30 s and a spinning rate of 5 kHz.  $^{27}\text{Al}$  MAS NMR spectra

were recorded at 104.26 MHz using very short,  $10^\circ$  powerful radiofrequency pulse delays with an interpulse delays of 0.5 s and a spinning rate of 15 kHz. The chemical shifts are quoted in ppm from external TMS (tetramethylsilane) and  $\text{Al}(\text{H}_2\text{O})_6^{3+}$ , respectively.

### 3 Results and discussion

#### 3.1 Characterisation of the particle suspensions

The dispersion ability of the precipitated powders was evaluated by measuring the zeta potential as a function of pH. The electrophoretic behaviours of the silicon containing species and aluminium-containing species precipitated separately at  $\text{pH } 8.25 \pm 0.25$  have been reported earlier.<sup>4</sup> The isoelectric points were located at pH values  $\approx 1.15$  and  $\approx 9.5$ , respectively.

Different values of IEP are cited in the literature for alumina and silica, depending on the crystallographic form, hydration state and history of the sample. The IEP of alumina may be contained in the pH range from 5 to 9.25.<sup>5</sup> However, a pH around  $9 \pm 0.2$  is most commonly reported<sup>6-8</sup> which is very close to the measured value. The IEP of silica has been variously reported to be from pH 0.5 to 3.75. Iler<sup>9</sup> reported that, in extensive studies of silica polymerisation, ion-exchange, and electrophoresis, an IEP between 1 and 1.5 was found, and that condensation was slowest there. The measured IEP for the silicon-containing species is in good agreement with these findings. Zeta potential values greater than  $\pm 25$  mV were registered for alumina and silica components species at pH values lower than 7 and higher than about 5.5, respectively. So, a strong mutual attractive interaction between the different particles of these two components is expected to occur when both are present in the suspensions.

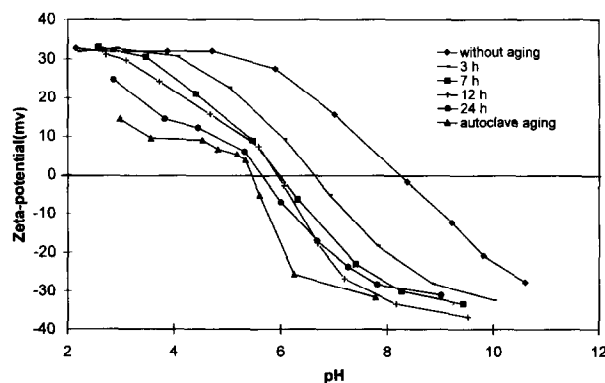


Fig. 1. The ageing effect on the electrophoretic behaviour of the coprecipitated powder.

The electrophoretic behaviours and the size distributions of particles in the unaged and aged suspensions for different times are shown in Figs 2 and 3, respectively. It can be observed that, at 100°C, increasing the ageing time leads to a decrease in the isoelectric point, while the average particle size shows only slight fluctuations. The IEP was further decreased by the autoclave treatment at 230°C for 72 h, whereas the average particle size continued almost unaffected. The shift

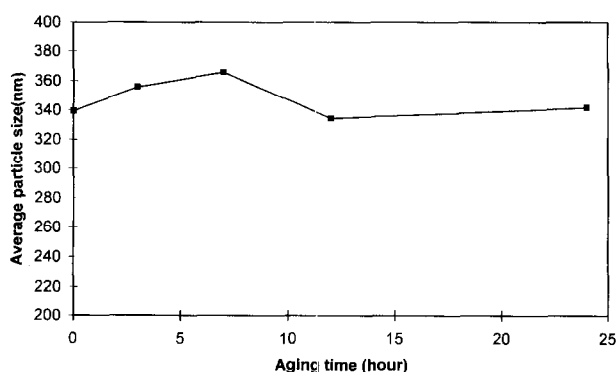


Fig. 2. The effect of the ageing time on particle (agglomerate) size distribution.

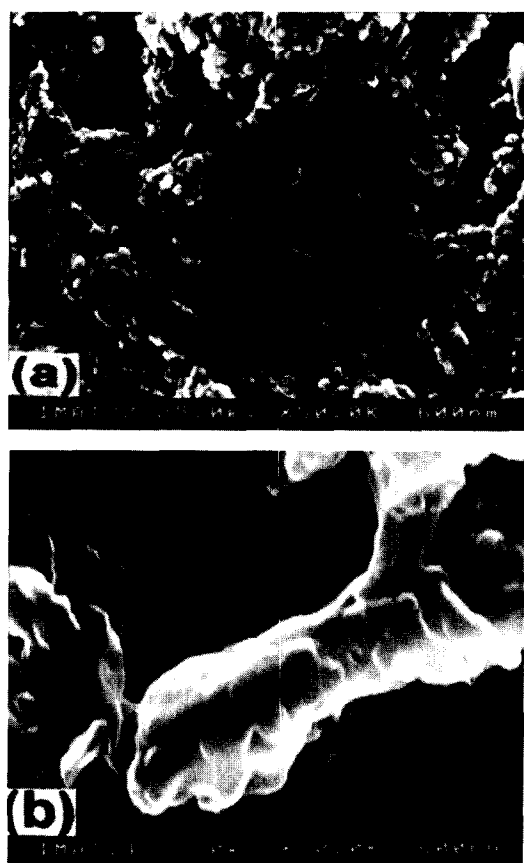


Fig. 3. The effect of the autoclave ageing on powder morphology (a) unaged, (b) autoclave aged at 230°C (72 h).

in IEP of about 3 pH units can be interpreted as an enrichment of the surface of the particles in silica species<sup>4</sup> promoted by depolymerization and dissolution precipitation processes resulting from the higher solubility of the silica species and from its tendency to be strongly adsorbed onto the surface of the hydrous aluminium oxides.<sup>1</sup> A decrease in the hydrated state can also have a minor influence.<sup>10</sup>

The pH of the coprecipitation medium when making the mullite with 10 vol% excess Al<sub>2</sub>O<sub>3</sub> was almost coincident with the IEP of the alumina component and, therefore, due to the attractive van der Waals forces, primary particles readily agglomerate, as can be observed in Fig. 3(a). So, the values presented in Fig. 2 should represent the size of the agglomerates. Figure 3(b) shows that the interparticle connections were reinforced by the dissolution precipitation process which occurred during ageing. The observed smoother surface of the aggregates can also result by a process of mass migration from the regions with high surface curvature to the regions with low or negative surface curvature, i.e. in the necks between two neighbouring particles,<sup>11</sup> which results in a reduction of surface area of the particles in the suspension. The decrease in IEP and surface area of the particles seem to be interesting features which will improve the colloidal processing ability of the coprecipitated powders by diminishing the tendency for particle aggregation.

### 3.2 Characterisation of powders

XRD spectra of the powders obtained from the freshly precipitated and from the refluxed suspensions at 100°C were practically coincident, indicating that, although this treatment strongly affected the surface properties of the particles, it did not interfere with their internal crystallographic structure. XRD spectra of the powders obtained from unaged and autoclave aged suspension are shown in Fig. 4. It can be observed that all bayerite phase present in the initial precursor was transformed into boehmite by the autoclave ageing treatment. This transformation was accompanied by a noticeable change in weight loss from 35.6%, measured for the unaged sample, to 22.4% for the autoclave treated powder, as shown by TG analysis in Fig. 5. The weight loss experienced by the powder aged at 100°C for 24 h attained the intermediate value of 30.2%. Since the crystalline structure of this powder was not substantially modified by the ageing treatment, the weight loss observed should be attributed to the condensation of the amorphous phases. The condensation process continues during

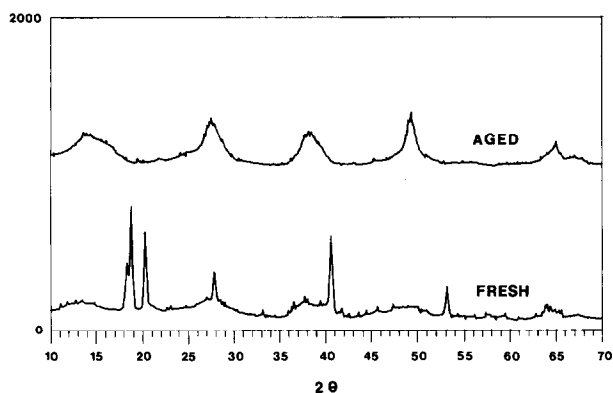


Fig. 4. XRD spectra of the precursors: (a) freshly prepared, (b) autoclave aged at 230°C (72 h).

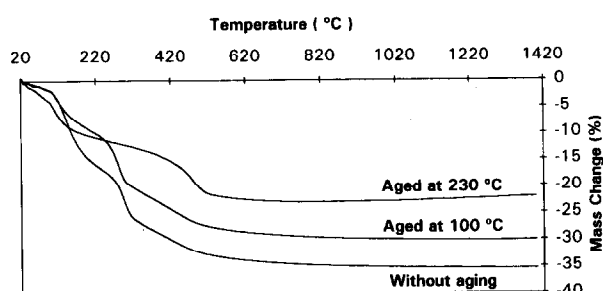


Fig. 5. TG curves of the precursors: (a) freshly prepared, (b) refluxed at 100°C (24 h), (c) autoclave aged at 230°C (72 h).

thermal treatment and is responsible for a broad exothermic peak, observed in the DTA curve of the unaged precursor, extending from 300 to 1000°C attributed to the crystallisation of the alumina and the condensation of the amorphous phase.<sup>3,12–14</sup>

The  $^{27}\text{Al}$  MAS NMR spectra of the unaged and aged precursors are shown in Fig. 6. Without ageing, the precursor shows two  $^{27}\text{Al}$  resonances, one at 56 ppm and another at about 8 ppm which can be attributed to the tetrahedral and octahedral coordination, respectively. The tetrahedral coordination of Al (very weak peak at 56 ppm) is due to aluminium in the nearest neighbour environment of silicon due to the atomic-scale mixing.<sup>15</sup> The  $^{27}\text{Al}$  resonance at  $\approx 8$  ppm represents Al in octahedral coordination due to the presence of the boehmite phase in the precursor which has all the Al in octahedral coordination.<sup>16</sup> After autoclave ageing, the two  $^{27}\text{Al}$  peaks shift to 69 ppm and 5 ppm, respectively. This is attributed to the dehydration and the changes of the polymerisation states, and the relative intensity of the resonance at 69 ppm which corresponds to the tetrahedral coordination is stronger than the resonance at 56 ppm from the unaged precursor. The shifts observed

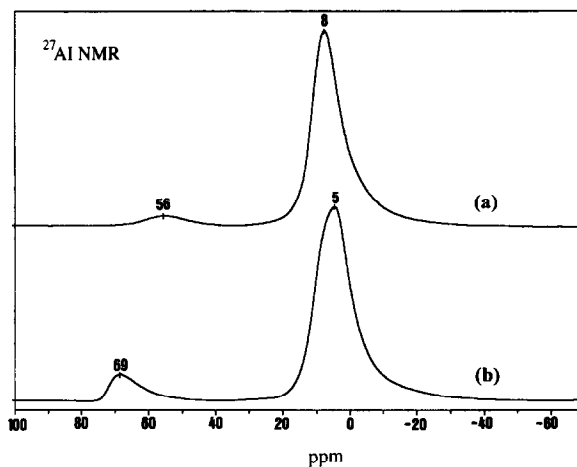


Fig. 6.  $^{27}\text{Al}$  MAS NMR spectra of the precursors: (a) freshly prepared, (b) autoclave aged at 230°C (72 h).

suggest that the percentage of Al ions in the nearest neighbour environment of silicon in the autoclave aged precursor is higher than that in the unaged precursor.

The  $^{29}\text{Si}$  MAS NMR spectra of the unaged and aged precursors are shown in Fig. 7. The spectrum of the unaged precursor showed broad complex peaks ranging from  $-80$  ppm to  $-120$  ppm. Therefore, they were considered to consist of a number of overlapped peaks. This indicates that there were various polymerisation states in the  $\text{SiO}_4$  tetrahedra of this precursor. The two strongest peaks are around  $-86$  ppm and  $-107$  ppm. The  $-86$  ppm peak can be assigned to  $\text{Q}^1$  or  $\text{Q}^2$  for  $\text{SiO}_4$  which could be  $\text{Q}^4(3\text{Al})$  or  $\text{Q}^4(2\text{Al})$  structures and the  $-107$  ppm peak can be assigned to  $\text{Q}^3$  or  $\text{Q}^4$  structures, where  $\text{Q}^1$ ,  $\text{Q}^2$  and so on refer to commonly accepted notations.<sup>17</sup> After autoclave ageing, the peaks around  $-107$  ppm which correspond to the

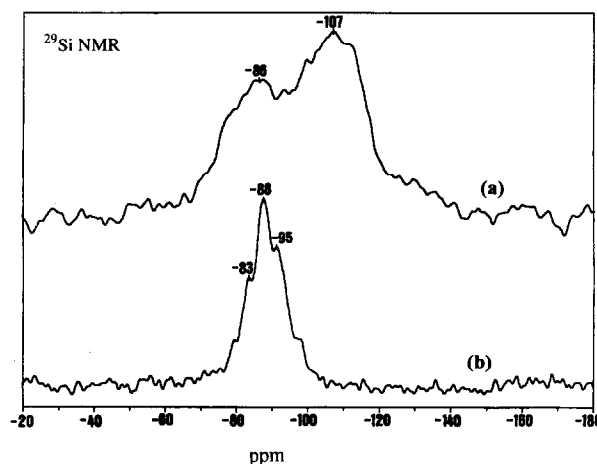


Fig. 7.  $^{29}\text{Si}$  MAS NMR spectra of the precursors: (a) freshly prepared, (b) autoclave aged at 230°C (72 h).

high polymerised silica disappear, all the resonances shift to lower fields around the strongest peak  $-88$  ppm, from  $-79$  ppm to  $-98$  ppm. Two different phenomena may contribute to this shifting of the resonance lines:<sup>18</sup> (i) the depolymerization of silica species (breaking of siloxane bonds,  $\equiv\text{Si}-\text{O}-\text{Si}\equiv$ , and formation of silanol groups,  $\equiv\text{Si}-\text{OH}$ ) which results in a shift of ca 10 ppm; (ii) replacement of  $\equiv\text{Si}-\text{O}-\text{Si}\equiv$  bonds by  $\equiv\text{Si}-\text{O}-\text{Al}\equiv$  bonds resulting in a chemical shift of ca 5 ppm. Combining the information obtained from electrophoresis and from the  $^{27}\text{Al}$  MAS NMR and  $^{29}\text{Si}$  MAS NMR spectra it seems reasonable to conclude that both phenomena should occur. In fact, the shift in IEP of about 3 pH units was attributed to an enrichment of the surface of the particles in silica species<sup>4</sup> promoted by depolymerization and dissolution precipitation processes resulting from the higher solubility of the silica species and from its tendency to be strongly adsorbed onto the surface of the hydrous aluminium oxides.<sup>1</sup> On the other hand, the  $^{29}\text{Si}$  MAS NMR spectra of the aged precursor is characteristic of a crystallised sample with well defined sites around  $-88$  ppm. A peak at  $-88$  ppm has been observed for homogeneous samples prepared by slow hydrolysis of aluminium and silicon alkoxides and was attributed to  $\text{Q}^4(2\text{Al})$  or  $\text{Q}^4(3\text{Al})$ .<sup>15</sup> So, both  $^{27}\text{Al}$  MAS NMR and  $^{29}\text{Si}$  MAS NMR spectra point out for an increasing mixing degree at the molecular level of the alumina and silica species in the autoclave aged sample.

The dehydration of the precursor, the displacement of the IEP to lower pH values and the increase of zeta potential in the alkaline region, the smoothing of the particle surface in the suspension with the concomitant reduction in the specific surface area, rendering the particles less active towards aggregation, constitute promising aspects for the desired improvement in colloidal processability of the slurries obtained by coprecipitation. On the other hand, the replacement of siloxane bonds by  $\equiv\text{Si}-\text{O}-\text{Al}\equiv$  bonds promoted by the autoclave ageing treatment also improves the degree of mixing of both components in the precursor.

#### 4 Conclusions

The following conclusions can be drawn from the data presented in this work:

1. With the increase in ageing time, the IEP of the particles in the suspensions decreases. This is interpreted as being mainly due to the

depolymerization and dissolution of the polymeric silica units and its deposition at particles surface. The mass migration from the regions with high surface curvature to the regions with low or negative surface curvature leads to the smoothing of the particles surface in the suspension and to a decrease of the specific surface area of the suspended powder.

2. The autoclave treatment transforms all bayerite phase present in the initial precursor into boehmite. This transformation is consistent with the observed change in weight loss of the unaged and aged precursors. The information obtained by MAS NMR spectra analysis reveals that the autoclave ageing involves dehydration, depolymerization, and replacement of  $\equiv\text{Si}-\text{O}-\text{Si}\equiv$  bonds by  $\equiv\text{Si}-\text{O}-\text{Al}\equiv$  bonds. After autoclave ageing the precursor becomes more homogeneous.

#### Acknowledgements

The authors would like to thank the NMR Laboratory of the University of Aveiro for performing the NMR spectra, and to Dr João Rocha for the fruitful discussions about NMR results.

#### References

1. Sacks, M. D. Lee, H. W. and Pask, J. A., A review of powder preparation methods and densification procedures of fabricating high density mullite. In *Ceramic Transactions*, Vol. 6, Mullite and Mullite Matrix Composites, ed S. Somiya, R. F. Davis, and J. A. Pask. American Ceramic Society, Westerville, OH, 1990, pp. 167–207.
2. Aksay, I. A., Dabbs, D. M. and Sarikaya, M., Mullite for structural, electronic, and optical applications. *Journal of Am. Ceram. Soc.*, 1991, **74**(10), 2343–2358.
3. Zhou Minghua, Ferreira, J. M. F., Fonseca, A. T. and Baptista, J. L., Wet chemical synthesis of nanocomposite powders in mullite-alumina system. Presented to 3rd International Conference, Ceramic-Ceramic Composites, Mons Belgium, October 18–20 1994, *Silicates Industriels*, Tome LXI, 1996, pp. 249–252.
4. Zhou, Minghua, Ferreira, J. M. F., Fonseca, A. T. and Baptista, J. L., Coprecipitation and processing of mullite precursor phases. *Journal of Am. Ceram. Soc.*, 1996, **79**(7), 1756–1760.
5. Parks, G. A., The isoelectric points of solid oxides, solid hydroxides, and hydroxo complex systems. *Chem. Rev.*, 1965, **65**, 177–198.
6. Velamakanni, B. F. and Lange, F. F., Effect of interparticle potentials and sedimentation on particle packing density of bimodal particle size distributions during pressure filtration. *Journal of Am. Ceram. Soc.*, 1991, **74**(1), 166–172.
7. Hunter, R. J., *Zeta Potential in Colloid Science-Principles and Applications*. Chapter 6.4. Academic Press, London, 1981.

8. Rao, A. S., Electrophoretic mobility of alumina, titania and their mixtures in aqueous dispersions. *Ceramics International*, 1988, **14**(2), 71–76.
9. Iler, R. K., *The Chemistry of Silica*, Chapter 3, refs 48, 52, 53, 57, Wiley-Interscience, New York, 1979.
10. Caldeira, P. A., Correia, R. N. and Baptista, J. L., Characterization, packing and sintering of chemically prepared mullite powders. In *Ceramics Today — Tomorrow's Ceramics — Materials Science Monographs*, Vol. 66B, Part B, ed P. Vincenzini. Elsevier, Amsterdam, 1991, pp. 871–880.
11. Wijnen, P. W. J. G., Beelen, T. P. M., Rummens, K. P. J., Saeijs, H. C. P. L., De Haan, J. W., De Ven, L. J. M. V. and Santen, R. A. V., The molecular basis of aging of aqueous silica gel. *Journal of Coll. Inter. Sci.*, 1991, **145**, 17–32.
12. Hyatt, M. J. and Bansal, N. P. J., Phase transformations in xerogels of mullite composition. *Mat. Sci.*, 1990, **25**, 2815–2821.
13. Lee, J. S. and Yu, S. C., Characteristics of mullite prepared from co-precipitated  $3\text{Al}_2\text{O}_3 \cdot 2\text{SiO}_2$  powders. *Journal of Mat. Sci.*, 1992, **27**, 5203–5208.
14. Dwivedi, R. K. and Gowda, G., Thermal stability of aluminium oxides prepared from gel. *Journal of Mat. Sci. Letters*, 1985, **4**, 331–334.
15. Takayuki Ban, Shigeo Hayashi and Atsuo Yasumori, Kiyoshi Okada, Characterization of low temperature mullitization. *Journal of Eur. Ceram. Soc.*, 1996, **16**, 127–132.
16. Komarneni, S. and Rutiser, C., Single-phase and diphasic aerogels and xerogels of mullite: preparation and characterization. *Journal of Eur. Ceram. Soc.*, 1996, **16**, 143–147.
17. Engelhardt, G. and Michel, D., *High Resolution Solid-State NMR of Silicates and Zeolites*. Wiley, New York, 1987, pp. 76–77.
18. Jaymes, I. and Douy, A., New aqueous mullite precursor synthesis. Structural study by  $^{27}\text{Al}$  and  $^{29}\text{Si}$  NMR spectroscopy. *Journal of Eur. Ceram. Soc.*, 1996, **16**, 155–160.